

Adsorption equilibrium of water vapor on activated carbon and alumina and carbon and alumina impregnated with hygroscopic salt

Ioan SOLOMON,¹ Ana M. RIBEIRO,² João C. SANTOS,² José M. LOUREIRO,²
Alírio E. RODRIGUES,² Ion SANDU³, Ioan MĂMĂLIĞĂ^{1,*}

¹Department of Chemical Engineering, Faculty of Chemical Engineering and Environmental Protection, “Gheorghe Asachi” Technical University of Iasi, 700050 Iasi, Romania

²Laboratory of Separation and Reaction Engineering, Department of Chemical Engineering, Faculty of Engineering, University of Porto, 4200-465 Porto, Portugal

³Arheoinvest Interdisciplinary Platform, “Alexandru Ioan Cuza” University of Iasi, 700506 Iasi, Romania

Received: 19.06.2012 • Accepted: 16.02.2013 • Published Online: 10.06.2013 • Printed: 08.07.2013

Abstract: The adsorption equilibrium of water vapor on different adsorbent materials has been studied. Small grains of commercial activated carbon and alumina, with a diameter of $d_g = 1.5 \times 10^{-3}$ m, were impregnated with a hygroscopic salt (calcium chloride) to improve the performance of these materials. The main characteristics of the new composite materials were obtained by adsorption/desorption of nitrogen at 77 K and salt distribution on the adsorbent surface was shown using scanning electron microscopy. The adsorption equilibrium isotherms of water vapor were measured by a gravimetric system at 2 different temperatures in the case of alumina and impregnated alumina (303 K and 313 K) and 1 temperature (303 K) in the case of activated and impregnated carbon. The impregnated material samples presented the highest adsorption capacity on the entire pressure range. The experimental points obtained for the activated carbon and alumina and the impregnated alumina were fitted with the Dubinin–Astakhov equation while the Langmuir equation was used to fit the impregnated carbon data.

Key words: Adsorption equilibrium, calcium chloride, water vapor, impregnated alumina, impregnated carbon

1. Introduction

The rapid development of different processes in industry has attracted more and more attention to gas and vapor adsorption, becoming a key point in many process industries and in environmental protection.^{1–3} A point of interest in these processes is represented by humidity control, due to the moisture influence on the product quality.^{2,4} Adsorption has become the most widely used method for water vapor removal, because it is less energy-consuming than other dehydration methods.⁵

The adsorption process can be physical or chemical, physisorption being preferred as it allows a low-temperature regeneration of the adsorbent.⁴ Water vapor removal is widely applied using porous materials, micropores, and mesopores. Microporous materials have pores filled with sorbate, which makes them an effective dehydrating agent, while mesoporous materials adsorb consecutive layers of sorbate, making them useful in humidity control.^{6–8}

Studies about water vapor adsorption were done using activated carbon as the microporous adsorbent

*Correspondence: imamalg@ch.tuiasi.ro

and activated alumina as the mesoporous adsorbent.^{2,5,9–11} In recent years, a new class of porous materials with higher performances was discovered. These materials are a combination between a porous material and an inorganic salt.^{3,6,10,12} The introduction of salt into the material pores can be done using different methods, impregnation presenting the advantage of a large porosity of the final product.⁷

Performances of these new materials are determined with the aid of adsorption equilibrium, which gives information regarding the adsorption capacity and the influence of material impregnation over the adsorption capacity.³ At the same time, studies about how the adsorbent grain size influences the rate of adsorption were done.¹²

The aim of the present work is to study the adsorption of water vapor on different adsorbents. The tested adsorbents are 2 commercial adsorbents, an activated carbon and an activated alumina, and samples of these adsorbents impregnated with 15% mass of calcium chloride.

Most of the literature papers refer to adsorption equilibrium of water vapor on activated or impregnated materials with solutions containing more than 25 wt% salt, using regular grain shapes.^{3,6,12} In this study we used adsorbent grain with irregularly shaped particles. To improve the impregnation quality and to uniformly distribute the salt in the grain structure, a solution containing 15% calcium chloride was used.

Adsorption equilibrium of water vapor on these materials was determined for a humidity of up to 90%. The temperature and impregnation effects on the adsorption capacity were studied. For the activated alumina and carbon, and also for the impregnated alumina, the experimental data were correlated with the Dubinin–Astakhov model, while the experimental data for the impregnated carbon were correlated with the Langmuir model. The parameters for these models were obtained.

2. Materials and methods

2.1. Materials

The experimental study was done using pure water vapor and 2 different types of commercial adsorbents: grains of activated carbon and activated alumina with an average size of $d_g = 1.5 \times 10^{-3}$ m. Using these materials as host matrix, 2 composite materials, MCC1 and MCA1, were then obtained by impregnation with a hygroscopic salt (CaCl_2). The procedure for impregnation is described below. The activated carbon and alumina were dried in an oven at 200 °C for 4 h and then cooled in a desiccator down to room temperature. The solid calcium chloride (Merck, Darmstadt, Germany) was also dried in an oven for 2 h and then dissolved in distilled water in order to obtain a solution of calcium chloride at 15 wt%. The activated adsorbent was then immersed in this solution for 4 h and, afterwards, separated using filtration under vacuum at room temperature. The grains of the new composite material were dried for 4 h in an oven at 200 °C and, afterwards, cooled in a desiccator.¹³

Using a WTW Cond 315i conductivity meter, the salt content in the composite material was determined to be 13.55 wt% CaCl_2 for impregnated carbon and 14.45 wt% CaCl_2 for the impregnated alumina.

Analysis regarding the inorganic salt distribution on the adsorbent external surface and in its pores was done using the scanning electron microscopy method. Images were obtained using an electronic microscope, SEM VEGA II LSH (TESCAN, Brno, Czech Republic), coupled with a QUANTAX QX2 EDX detector (Bruker, Bremen, Germany). The results are presented in Figures 1 and 2.

The EDX detector is of the third-generation and does not require liquid nitrogen cooling, being about 10 times faster than conventional Si (Li) detectors. The microscope, entirely computer controlled, has an electron gun with a tungsten filament, which can achieve a resolution of 3 nm at 30 kV and a zoom range from $30 \times$ to $1,000,000 \times$, the acceleration voltage ranging between 200 V and 30 kV while the scanning speed is from 200

ns to 10 ms per pixel. Its working pressure is lower than 1×10^{-2} Pa. The resulting image can be formed by secondary electrons and backscatter electrons.

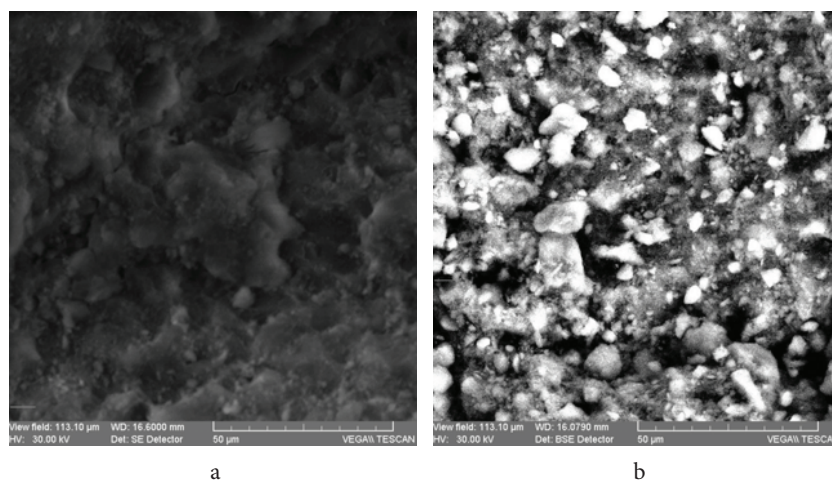


Figure 1. Scanning electron microscopy images for a) activated alumina and b) impregnated alumina.

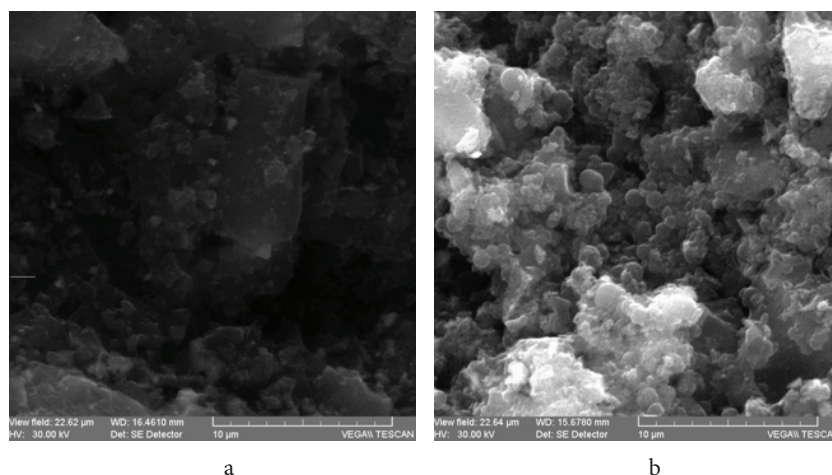


Figure 2. Scanning electron microscopy images for a) activated carbon and b) impregnated carbon.

Using the nitrogen adsorption/desorption isotherms at 77 K, the main characteristics of the new composite materials were determined. In this scope, an ASAP 2020 (Micromeritics, Norcross, GA, USA) was used in the case of impregnated alumina and an Autosorb 1 (Quantachrome Instruments, Boynton Beach, FL, USA) in the case of impregnated carbon. In Figure 3 the determined isotherms are shown, the main characteristics of materials being presented in Table 1. As can be seen in Figure 3a, the impregnated alumina gives a Type IV adsorption isotherm, according to IUPAC, with an initial rise at low relative pressure and the adsorbed volume increasing progressively with the relative pressure increase.¹⁴ In the range of relative pressure above 40%, the isotherm presents a pronounced hysteresis between the adsorption and desorption branches caused by the pore filling and emptying by capillary condensation, indicating the presence of mesoporosity. The impregnated carbon gives a Type I adsorption isotherm according to IUPAC and is presented in Figure 3b.¹⁴ Compared with the impregnated alumina isotherm, this isotherm shows a sharp rise at low relative pressures reaching an

almost constant plateau for higher values of relative pressure, indicating a very low external surface, which is specific for microporous materials.

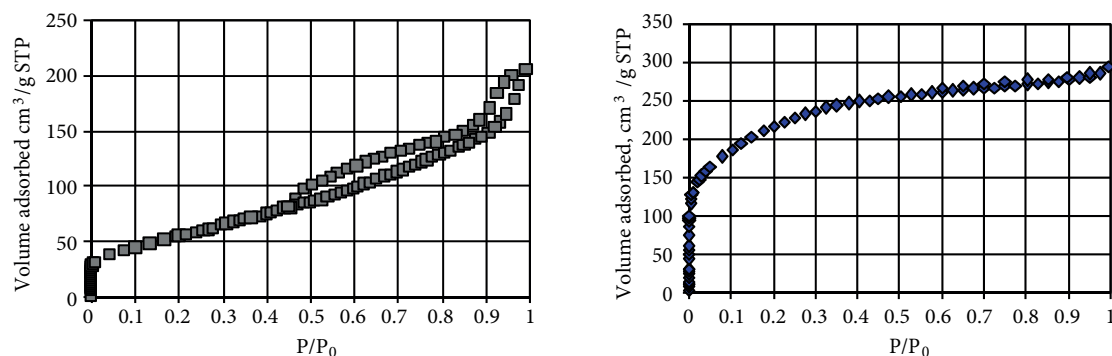


Figure 3. Nitrogen adsorption/desorption isotherms at 77 K for a) impregnated alumina and b) impregnated carbon.

Table 1. Main characteristics of the new composite materials.

Characteristics	Impregnated alumina	Impregnated carbon
Microporous volume, $\text{cm}^3 \text{g}^{-1}$	0.06	0.36
Mean pore size, nm	2.38	2.31
BET specific surface, $\text{m}^2 \text{g}^{-1}$	190	765
External specific surface, $\text{m}^2 \text{g}^{-1}$	216	56.1
Microporous specific surface, $\text{m}^2 \text{g}^{-1}$	50	708.6

2.2. Experimental methods

The determination of the water vapor adsorption isotherms was done using the gravimetric method with the experimental setup presented in Figure 4. A magnetic suspension balance with a precision of 0.01 mg (Rubotherm, Bochum, Germany) was used. Approximately 2 g of adsorbent was placed in a basket suspended by the permanent magnet of the balance. The balance was then covered with a cell jacket having temperature controlled by a thermostatic bath (Huber, Offenburg, Germany) to maintain an isothermal regime of the process.

The water vapor was supplied to the system from a tank made from stainless steel. The tank was immersed in a thermostatic bath (Lauda, Lauda-Königshofen, Germany). The temperature control of the tank bath allowed the generation of the required water vapor pressure. In order to have pure water vapor, a vacuum was first made in the tank, then liquid distilled water was introduced to the tank, and finally a vacuum was made again to degasify the water. To avoid condensation, all the tubes in the set-up were covered with a heating tape, which kept the temperature 2–4 °C higher than the experimental temperature.

A thermocouple and a pressure transducer (Sensortechnics, Puchheim, Germany) were connected to the balance exit to monitor the temperature and the pressure during the adsorption process. The temperature, the pressure, and the mass were acquired and recorded continuously.

Before starting the adsorption process, the adsorbent was activated by heating it to 413 K at a heating rate of 1 K min^{-1} and left under vacuum overnight. Helium pycnometry was used to determine the initial mass and volume of the adsorbent after activation.

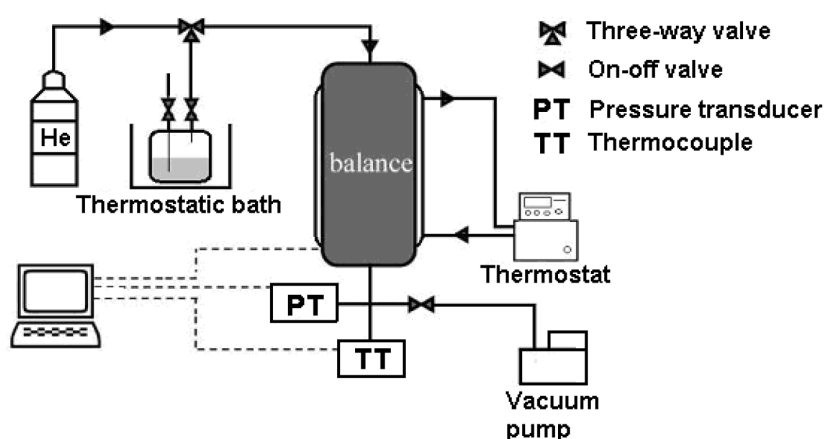


Figure 4. Adsorption equilibrium experimental set-up.

3. Results and discussion

The temperature and the impregnation influences on the material adsorption capacity were investigated using 4 materials at 2 different temperature values of 303 K and 313 K.

The experimental data were fitted using the Dubinin–Astakhov equation for activated carbon and alumina and impregnated alumina, and the Langmuir equation was used for impregnated carbon.¹⁵

The Dubinin–Astakhov equation is represented by Eq. (1):

$$q = q_m \exp \left\{ - \left[\frac{RT}{E} \ln \left(\frac{P_0}{P} \right) \right]^m \right\}. \quad (1)$$

The Langmuir equation is represented by Eq. (2):⁸

$$q = q_m \cdot \frac{b \cdot P}{1 + b \cdot P}, \quad (2)$$

$$b = b_\infty \cdot \exp \left(\frac{Q}{R \cdot T} \right). \quad (3)$$

In order to obtain the fitting parameters, deviations between experimental and calculated data were determined using Eq. (4) and, afterwards, they were minimized.

$$\Delta q, \% = \frac{100}{k} \cdot \sum_{j=1}^k \frac{(q_j^{\text{exp}} - q_j^{\text{calc}})^2}{q_j^{\text{exp}}}. \quad (4)$$

In the case of activated and impregnated alumina, the experimental data and the fitted isotherms are presented in Figure 5 for 2 temperature values, 303 K and 313 K, the fitting parameters being presented in Table 2. Type IV adsorption isotherms, according to IUPAC, were obtained for both materials.¹⁴ At low pressure values, the water molecules chemisorb to the adsorbent surface, while at higher pressure values they physisorb on the already chemisorbed molecules. As can be seen from these figures, the adsorption capacity is influenced by the temperature, a temperature increase leading to a decrease of the adsorption capacity.

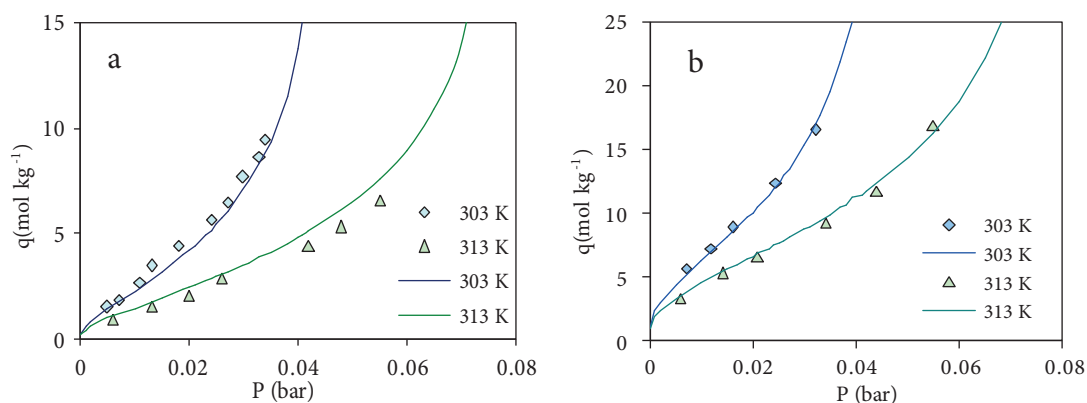


Figure 5. Adsorption isotherms of water vapor on a) activated alumina and b) impregnated alumina at \blacklozenge 303 K and \blacktriangle 313 K (points - experimental; lines - Dubinin–Astakhov fitting).

Table 2. Fitting parameters of the models for water vapor adsorption equilibrium on activated alumina, impregnated alumina, activated carbon, and impregnated carbon at 303 K and 313 K.

Material	Model	q_m (mol kg ⁻¹)	q_{sat} (mol kg ⁻¹)	m	b_∞	E (J mol ⁻¹)	Q (J mol ⁻¹)
Activated alumina	Dubinin–Astakhov	21.28	-	0.49	-	702	-
Impregnated alumina	Dubinin–Astakhov	44.86	-	0.42	-	730	-
Activated carbon	Dubinin–Astakhov	288.9	-	0.55	-	128	-
Impregnated carbon	Langmuir	-	66.41	-	4.15E-05	-	32,382

In Figure 6, the adsorption isotherms of activated alumina and impregnated alumina obtained at 313 K are compared. Points for both adsorption and desorption processes are shown. The strong influence of the impregnation on the adsorption capacity can be observed, the new composite material showing a remarkably better performance when compared to the basic matrix. The salt content also has an influence on the shape of the hysteresis, the loop being larger in the case of activated alumina than that obtained for the impregnated alumina.

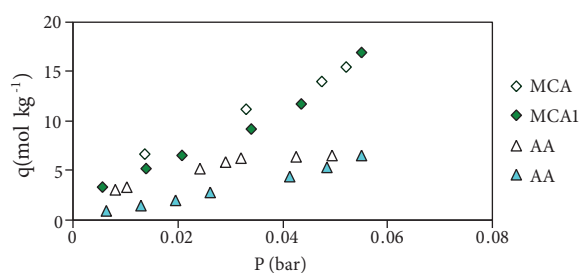


Figure 6. Adsorption isotherm of water vapor onto \blacklozenge impregnated alumina (MCA1) and \blacktriangle activated alumina (AA) at 313 K (filled symbols - adsorption; hollow symbols - desorption).

The experimental data for the adsorption equilibrium of water vapor on activated and impregnated carbon are presented in Figure 7 for the temperature of 303 K. The lines represent the fitted isotherms, with the parameters presented in Table 2 for activated carbon and for impregnated carbon.

As it can be seen from the 2 figures, the adsorption isotherm for activated carbon is Type III according to IUPAC and it can be described by the Dubinin–Astakhov equation, while the adsorption isotherm for impregnated carbon is Type I and is described by the Langmuir equation. The explanation for the different

shape of the 2 curves is the salt content in the case of impregnated carbon. While adsorption of water vapors on activated carbon occurs only by physical processes with weak interactions between the adsorbent and the adsorbate, in the case of impregnated carbon, adsorption of water vapors occurs both by physical and chemical processes. Considering the fact that the salt is highly hygroscopic, hydration is strong even at low values of pressure, while for higher values of pressure, the salt is saturated and the equilibrium is reached.

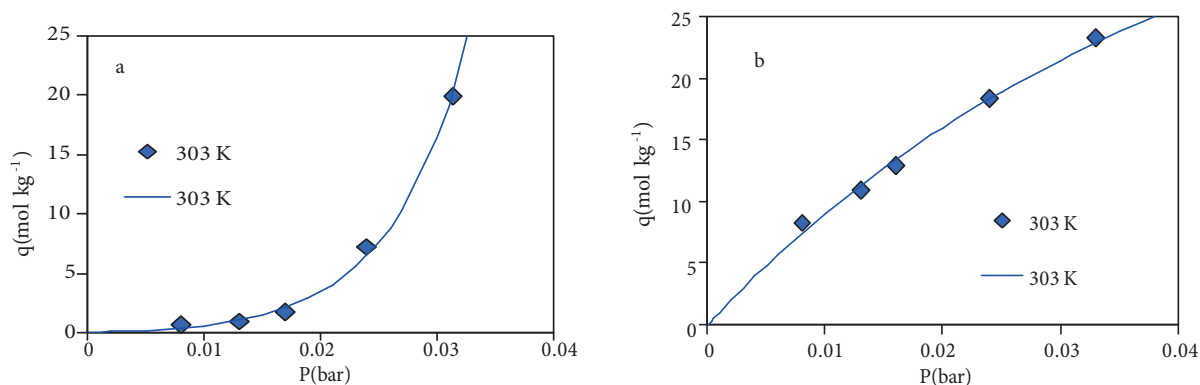


Figure 7. Adsorption isotherms of water vapor onto a) activated carbon and b) impregnated carbon at 303 K (points - experimental; lines - Dubinin–Astakhov and Langmuir fitting).

The effect of carbon impregnation over the adsorption capacity is also highlighted in this figure. As can be seen, the amount of water vapor adsorbed on impregnated carbon is significantly higher than for activated carbon, proving once again the influence of impregnation.

A comparison between the 4 adsorbent materials is made in Figure 8 for the results obtained at a temperature of 303 K. It is observed primarily that the impregnated materials have a higher affinity for water vapor than the basic matrix, due to the content in highly hygroscopic salt (CaCl_2), and secondly that the activated carbon, which is a microporous material, although it has weak interactions with water vapor, presents a higher adsorption capacity than that of mesoporous materials, represented in this case by activated alumina and impregnated alumina.⁸

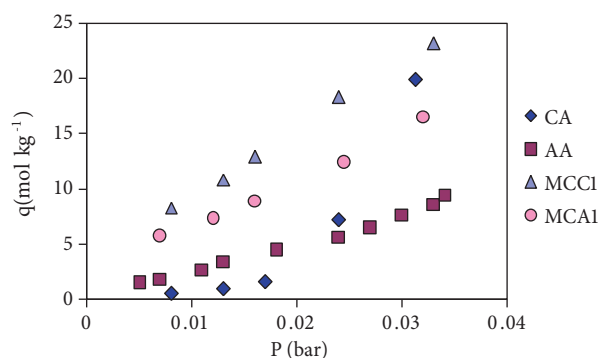


Figure 8. Adsorption isotherm of water vapor onto \blacklozenge activated carbon (CA), \blacktriangle impregnated carbon (MCC1), \blacksquare activated alumina (AA), and \bullet impregnated alumina (MCA1) at 303 K.

4. Conclusion

An experimental study of the adsorption equilibrium of water vapor on porous materials was done. The materials used are small grains ($d_g = 1.5 \times 10^{-3} \text{ m}$) of activated carbon, activated alumina, impregnated carbon, and

impregnated alumina. The composite materials were obtained by impregnation with a hygroscopic salt. The salt contents were determined to be 13.55 wt% CaCl_2 for the impregnated carbon and 14.45 wt% CaCl_2 for the impregnated alumina.

The experiments were carried out at 2 different temperatures in the case of activated alumina and impregnated alumina (303 K and 313 K) and 1 temperature (303 K) in the case of activated carbon and impregnated carbon.

It was demonstrated that with increasing temperature the adsorption capacity decreases, and that the impregnated materials present a much higher adsorption capacity in comparison to the basic materials (i.e. for the temperature of 303 K and a pressure of 0.024 bar, the adsorption capacity for the activated alumina is 5.7 mol kg^{-1} , while for the impregnated alumina and for the activated carbon, it is 12.4 mol kg^{-1} and 7.2 mol kg^{-1} , respectively, and, finally, for the impregnated carbon it is 18.3 mol kg^{-1}). It has also been shown that the impregnated carbon presents a higher affinity for water vapor than the activated and impregnated alumina, respectively.

Experimental data were fitted using different equations. For the cases of activated carbon and alumina and impregnated alumina, the Dubinin–Astakhov equation was used, and in the case of impregnated carbon, the Langmuir equation was used. The experimental data are in good agreement with the calculated data.

Acknowledgment

This work was done with the support of the EURODOC “Doctoral Scholarships for Research Performance at European Level” project, financed by the European Social Fund and Romanian Government.

Nomenclature

d_g	Grain diameter	$q^{\text{exp}}, q^{\text{calc}}$	Experimental and calculated adsorbed concentrations
k	Number of data points at a given temperature	E	Characteristic energy
m	Surface heterogeneity	Q	Heat of adsorption
q	Adsorbed concentration	R	Gas constant
q_m	Saturation adsorbed concentration	T	Temperature

References

- Deng, S. *In Encyclopedia of Chemical Processing*, Lee, S. Ed.; Taylor & Francis, New York, USA, 2006.
- Kim, J. H.; Lee, C. H.; Kim, W. S.; Lee, J. S.; Kim, J. T.; Suh, J. K.; Lee, J. M. *J. Chem. Eng. Data* **2003**, *48*, 137–141.
- Mamaliga, I.; Baciuc, C.; Petrescu, S. *Environ. Eng. Manag. J.* **2009**, *8*, 253–257.
- Nakabayashi, S.; Nagano, K.; Nakamura, M.; Togawa, J.; Kurokawa, A. *Adsorption* **2011**, *17*, 675–686.
- Serbezov, A. *J. Chem. Eng. Data* **2003**, *48*, 421–425.
- Okada, K.; Nakanome, M.; Kameshima, Y.; Isobe, T.; Nakajima, A. *Mater. Res. Bull.* **2010**, *45*, 1549–1553.
- Wang, L. W.; Wang, R. Z.; Oliveira, R. G. *Renew. Sustain. Energy Rev.* **2009**, *13*, 518–534.
- Rouquerol, F.; Rouquerol, J.; Sing, K.S.W. *Adsorption by Powders and Porous Solids: Principles, Methodology and Applications*, Academic Press, San Diego, USA, 1999.
- Oh, J. S.; Shim, W. G.; Lee, J. W.; Kim, J. H.; Moon, H.; Seo, G. *J. Chem. Eng. Data* **2003**, *48*, 1458–1462.
- Kim, M. B.; Ryu, Y. K.; Lee, C. H. *J. Chem. Eng. Data* **2005**, *50*, 951–955.
- Huggahalli, M.; Fair, J. R. *Ind. Eng. Chem. Res.* **1996**, *35*, 2071–2074.
- Glaznev, I. S.; Koptuyg, I. V.; Aristov, Y. I. *Micropor. Mesopor. Mat.* **2010**, *131*, 358–365.
- Secula, M. S.; Spiridon, M.; Solomon, I.; Petrescu, S. *Rev. Chim.* **2011**, *62*, 1175–1179.
- Keller, J. U.; Staudt, R. *Gas Adsorption Equilibria: Experimental Methods and Adsorptive Isotherms*, Springer, New York, USA, 2005.
- Do, D. D. *Adsorption Analysis: Equilibria and Kinetics*, Vol. 2, Imperial College Press, London, UK, 1998.